

Spatial pattern of $K_d(\text{PAR})$ and its relationship with light absorption of optically active components in inland waters across China

Zhidan Wen^a, Kaishan Song^{a*}, Chong Fang^a, Qian Yang^b, Ge Liu^a, Yingxin Shang^a,Xiaodi Wang^c

^aNortheast Institute of Geography and Agroecology, Chinese Academy of Sciences,
Changchun 130102, China

^bJilin Jianzhu University, Changchun 130118, China

^cHarbin university, Harbin 150086, China

*Corresponding author, E-mail: songks@neigae.ac.cn

Northeast Institute of Geography and Agroecology, Chinese Academy of Sciences,
Changchun 130102, China

Abstract

The spatial distribution of the attenuation of photosynthetic active radiation ($K_d(\text{PAR})$) was routinely estimated in China lakes and reservoirs. Higher mean value of $K_d(\text{PAR})$ was observed in Northeastern plain and mountainous region (NER). A linear model is used to predict $K_d(\text{PAR})$, as a function of light absorption coefficient of pigment particulates (a_{phy}), colored dissolved organic matters (a_{CDOM}), and inorganic particulate matters (a_{NAP}): $K_d(\text{PAR}) = 0.41 + 0.57 \times a_{\text{CDOM}} + 0.96 \times a_{\text{NAP}} + 0.57 \times a_{\text{phy}}$ ($R^2 = 0.87$, $n = 741$, $p < 0.001$). Spatial $K_d(\text{PAR})$ was relatively dependent on the inorganic particulate matters (average relative contribution of 57.95%). When only consider the contribution of absorption of a_{OACs} to $K_d(\text{PAR})$, the results highlight that the a_{OACs} could explain 70%-87% of $K_d(\text{PAR})$ variations. In the lakes with low TSM concentration and non-eutrophic lakes with high TSM, a_{CDOM} was the most powerful predicting factor on $K_d(\text{PAR})$. In eutrophic lakes with high TSM, a_{NAP} had the most significant impact on $K_d(\text{PAR})$. This study allowed $K_d(\text{PAR})$ to be predicted from a_{OACs} values in the inland waters. Besides, results of this study are suggesting that new studies on the variability of $K_d(\text{PAR})$ in inland waters must consider the hydrodynamic conditions, trophic status and the distribution of optically active components within the water column.

Keywords: light attenuation, light absorption, optically active components, photosynthetic active radiation, inland waters

1. Introduction

Light is one of the most important factors governing primary production and photosynthesis in the aquatic ecosystems (Kirk, 1994; Ma et al., 2016; Song et al., 2017). Light availability plays a crucial role in the distribution of phytoplankton and hydrophytes, and it is also a good indicator of the trophic status of an aquatic system. Photosynthetically active radiation (PAR) for phytoplankton growth is a product of the input of solar radiation at the surface and its reduction by optically active components (OACs) through absorption and scattering (Devlin et al., 2009). The diffuse attenuation of photosynthetic active radiation ($K_d(\text{PAR})$) is commonly used to quantitatively assess the light availability, it indicates the ability of solar radiation to penetrate a water column (Kirk, 1994). $K_d(\text{PAR})$ can be obtained by the profile of PAR values measured at different water depths according to Lambert-Beer's law (Devlin et al., 2009; Devlin et al., 2008; Shi et al., 2014). However, in situ measurements of $K_d(\text{PAR})$ in waters have obvious limitations, and it is difficult to achieve spatial coverage. Satellite remote sensing has achieved the mapping of $K_d(\text{PAR})$ distribution from various types of satellite remote sensing data in open sea, coastal and inland waters in recent years (Chen et al., 2015; Shi et al., 2014; Song et al., 2017). However, Environmental change and anthropogenic activity have made it challenging to accurately assess K_d patterns in the extremely turbid inland waters (Zheng et al., 2016). The comprehensive analysis of the relationships between $K_d(\text{PAR})$ and a_{OACs} is an imperative requirement to retrieve $K_d(\text{PAR})$ from remote sensing data for turbid inland waters (Ma et al., 2016).

A number of components in water contribute to the attenuation of light, including water itself, colored dissolved organic matters (CDOM), phytoplankton pigment particles (expressed here as the concentration of chlorophyll-*a*), and inorganic suspended particles (Prieur & Sathyendranath, 1981). Water and CDOM absorb light,

pigment and inorganic particles absorb and scatter light (Effler et al., 1985; Shi et al., 2014). Absorption and scattering by these OACs are the main attenuation factors of $K_d(\text{PAR})$ in the water (Budhiman et al., 2012; Zheng et al., 2016). The relative contribution of OACs to $K_d(\text{PAR})$ have researched in numerous studies previously in lakes, estuaries and offshore waters (Brandao et al., 2017; Lund-Hansen, 2004; Phlips et al., 1995b; V-Balogh et al., 2009; Yamaguchi et al., 2013), there is general agreement by now that inorganic suspended particles had the decisive effect on light attenuation in turbid waters (Brandao et al., 2017; Yang et al., 2005; Zhang et al., 2007a). In transparent marine and freshwater systems, phytoplankton is also an important component in PAR attenuation (Laurion et al., 2000; Lund-Hansen, 2004). Studies about $K_d(\text{PAR})$ partition and the influencing factors provide important information to predict the underwater light climate from the concentrations of these factors (Brandao et al., 2017; Zhang et al., 2007b). In present, the contribution of OACs to light attenuation in many studies included both OACs absorption (a_{OACs}) and particulates scattering. In fact, the particulates scattering occupied small proportion of total contribution, most of the light attenuation in water was induced by a_{OACs} (Belzile et al., 2002). Thus, the relationship between $K_d(\text{PAR})$ and a_{OACs} is very essential to predict $K_d(\text{PAR})$ based on a_{OACs} in inland waters.

Although $K_d(\text{PAR})$ characterization has been carried out in various aquatic environments, including freshwater, estuaries, coastal water, and open ocean water (Belzile et al., 2002; Cunningham et al., 2013; Frankovich et al., 2017; Lund-Hansen, 2004; Zhang et al., 2007a), few studies have been performed in the extremely turbid waters and plateau water with strong ultraviolet radiation (Ma et al., 2016; Shi et al., 2014; Song et al., 2017). In transparent marine and freshwater systems, phytoplankton was suggested to be an important component in light attenuation (Brandao et al., 2017;

Yang et al., 2005). However, in turbid inland waters, the components of OACs vary independently (Matsushita et al., 2015; Wen et al., 2016), and studies have pointed out that the components of OACs had large spatial and temporal variations in turbid inland waters (Oliver et al., 2017; Zhang et al., 2018; Zhao et al., 2016). The governing factors controlling $K_d(\text{PAR})$ always changed with the OACs concentration and component in different inland waters (Brandao et al., 2017; Cunningham et al., 2013; Laurion et al., 2000). China has a large number of inland waters, and they exhibit large variability in terms of the optical properties and trophic status. A large proportion of lakes in China are characterized by highly turbid waters (Song et al., 2018). Thousands of closed lakes with high salinity have developed in the plateau area, and they are exposed to high intensity solar radiation (Laurion et al., 2000; Ma et al., 2011). To the best of our knowledge, there is little work has analyzed in detail the effect of a_{OACs} on $K_d(\text{PAR})$ in a large variety of inland waters across China.

In this study, our objectives were (1) to describe the spatial distribution of $K_d(\text{PAR})$ in five limnetic regions, China; (2) evaluate which optical variables control the $K_d(\text{PAR})$ in the water column of inland waters, especially in the different types of lakes, (3) to provide an empirical model to estimate $K_d(\text{PAR})$ in these inland waters. The study is essential to remote sensing of $K_d(\text{PAR})$ and evaluate the underwater light climate.

2. Materials and Methods

2.1. Study area and Sampling description

China is situated in eastern Asia, covering an area of approximately $9.6 \times 10^6 \text{ km}^2$ (E: $73^\circ 40' - 135^\circ 2' 30''$, N: $3^\circ 52' - 53^\circ 33'$). There are a large number of lakes and reservoirs with the total surface area of $104,415 \text{ km}^2$, accounting for 3.48% of the global lake and reservoir surface area (Ma et al., 2011; Raymond et al., 2013; Wen et al., 2017). In accordance with the regions and topography, the lakes are divided into five limnetic

regions: Inner Mongolia -Xinjiang plateau region (MXR), Tibet-Qinghai Lake Region (TQR), Northeastern plain and mountainous region (NER), Yunnan- Guizhou Plateau region (YGR), and Eastern plain region (ER) (Wen et al., 2017). The trophic status of lakes in China included oligotrophic, mesotrophic, and hypereutrophic, water quality of the majority of lakes has degraded (Jin et al., 2005).

A total of 13 field surveys were carried out between April 2015 and September 2017 with a total of 741 locations covered 141 lakes and reservoirs in China (here after together called lakes) (Figure 1). The areas of these lakes ranged from 1 km² to 3,283 km². These lakes distributed in different climatic zones with various land-use types. During the sampling period the mean day air temperatures ranged from 15 to 25 °C. The surface water (0.2-0.5 m depth) was collected in the acid-washed HDPE bottles, and were placed in a portable refrigerator before they were carried back to the laboratory. Water samples were collected at 5-7 sampling points from lakes on average, in the meanwhile, PAR values were also measured in the same point. The PAR values were measured using the LI-COA 193SA underwater spherical quantum sensor. The operation was conducted on the sunny side of the boat to avoid any shadow effects. The PAR measurements were taken at no less than five point's depth for each station. At each depth in the water, PAR value was continuously recorded for 15 s and output an averaged value, the average value was regarded as the PAR value at this water depth (Ma et al., 2016).

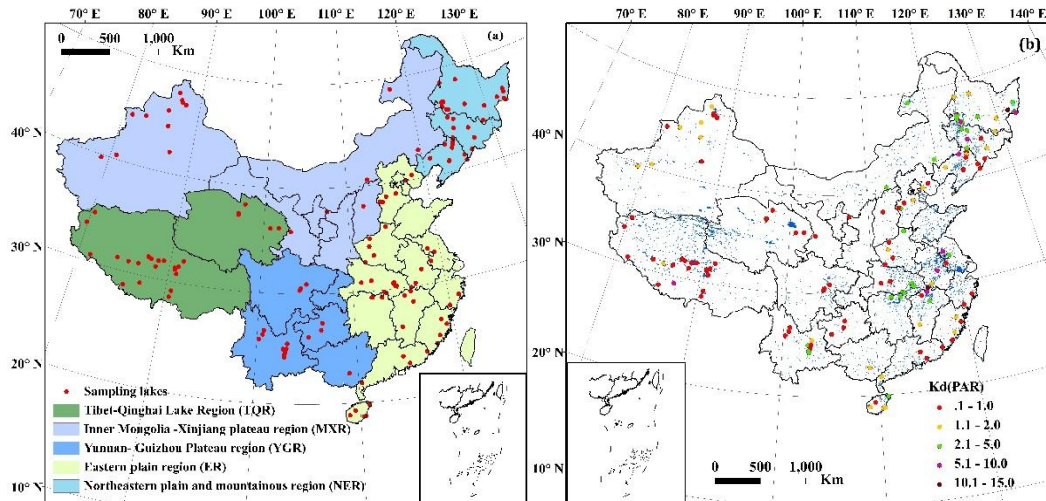


Fig. 1 Study area location and sampling lakes distribution, (a) sampling lakes distribution in five limnetic regions, (b) $K_d(\text{PAR})$ values distribution of every sampling lake

2.2. Water quality and light absorption parameters measurement

Salinity and pH were measured by a portable multi-parameter water quality analyzer (YSI 6600, U.S) in situ with the uncertainty of 0.01 ppt and 0.01, respectively. Secchi disk depth (SDD) at each sampling point was measured using a 30 cm diameter Secchi disk. All water samples were filtered through 0.45 μm mixed fiber millipore filters within 24 h of sampling, and the filtered waters were used to TN concentrations analysis by a continuous flow analyzer (SKALAR, San Plus System, the Netherlands). Total phosphorus (TP) was determined using the molybdenum blue method after the samples were digested with potassium peroxydisulfate (APHA et al., 1998). DOC concentrations were also analyzed using a total organic carbon analyzer (TOC-VCPN, Shimadzu), details can be found in the reference (Song et al., 2018). Chlorophyll a (*Chla*) was extracted from raw water samples using a 90% buffered acetone solution, and the concentration was determined by spectrophotometry (UV-2600 PC, Shimadzu) (Jeffrey & Humphrey, 1975). Total suspended matter (TSM) concentration was determined gravimetrically, a certain volume of raw water were filtered through pre-combusted 0.7 μm glass fiber millipore filters (Whatman, GF/F 1825-047), the

particulate matter were retained in the filters, and then the filters were combusted for 2h on 400°C. TSM concentration was calculated by the difference between filtered combusted filter and non- filtered combusted filter (Cleveland & Weidemann, 1993).

Total particulate light absorption (a_p) of the filter captured TSM was determined by UV spectrophotometry (Shimadzu, 2660) with a virgin filter as a reference (Cleveland & Weidemann, 1993). Then the sodium hypochlorite solution was used to remove pigments in this filter, and the bleached filter was determined again to obtain the optical density (OD_λ) of the non-algal particles (a_{NAP}). The pigment or phytoplankton light absorption coefficient (a_{phy}) was the difference between a_p and a_{NAP} . The collected water samples were filtered in turn through a GF/F 0.7 μm glass fiber membrane and a 0.2 μm polycarbonate membrane to extract CDOM. The filtering process should be finished within 24 h away from light. Light absorption of colored dissolved organic matter (a_{CDOM}) in the waters was also measured using a UV-2600 spectrophotometer equipped a 5 cm quartz cuvette, the Milli-Q water was used as a reference. The light absorption coefficient of CDOM at 700 nm was used to correct CDOM absorption coefficients to eliminate the internal back scattering (Bricaud et al., 1981). The absorption coefficients (a_p , a_{phy} and a_{CDOM}) were derived from the measured OD_λ as the following equations (Bricaud et al., 1981; Bricaud & Stramski, 1990). In this study, absorption coefficients at 440 nm was chosen for analysis later in this study (Wen et al., 2016). The light absorption of optically active components (a_{OACs}) is the sum of a_{CDOM} and a_p . Where $a_{CDOM}(\lambda)$, $a_p(\lambda)$, and $a_{phy}(\lambda)$ are the CDOM, total particulate and phytoplankton absorption coefficients at a given wavelength, respectively; L is the cuvette path length (0.01 m); S is the effective area of the deposited particle on the fiber membrane (m^2); V is the volume of the filtered water (m^3); 2.303 is the conversion factor; and $OD_{(null)}$ is the OD value at 700 nm.

$$a_{CDOM}(\lambda) = 2.303 \times [OD_{(\lambda)} - OD_{(null)}] / L \quad (1)$$

$$a_p(\lambda) = 2.303 \times \frac{S}{V} \times OD_{(\lambda)} \quad (2)$$

$$a_{phy}(\lambda) = a_p(\lambda) - a_{NAP}(\lambda) \quad (3)$$

2.3. Data analysis

$K_d(PAR)$ was calculated using the exponential regression model as the following equation, where Z is the water depth, and PAR_Z is the photosynthetic active radiation value at depth Z (Pierson et al., 2008; Stambler, 2005). The results were accepted only if the coefficient of determination (R^2) was higher than 0.95.

$$PAR_{Z2} = PAR_{Z1} \times e^{-K_d(PAR) \times (Z2 - Z1)} \quad (4)$$

A classification regression tree approach (CHAID) was used to classify the lakes based on $K_d(PAR)$ in SPSS 19.0 (Breiman et al., 1984; Hampton et al., 2017). $K_d(PAR)$ was used value as the response variable, the explanatory variables were TSM, $Chla$, a_{CDOM} , pH, salinity, and trophic status of lakes. Mean value and standard error of $K_d(PAR)$ were calculated for each branch of the regression tree.

The assessment of the trophic status of lakes was based on the modified Carlson's trophic state index (TSI), using measured $Chla$, TP and SDD data (Carlson, 1977; Aizaki et al., 1981). The traditional TSI method used numbers (0-100) to express the state of a lake: $TSI < 30$ indicates oligotrophic state, 30 - 50 indicates mesotrophic state, and 50 - 100 indicates eutrophic state.

We approached data analysis in the following ways: First, the $K_d(PAR)$ differences in different limnetic regions across China were quantified by the regional mean value of all lakes. Meanwhile, the relative contributions of a_{OACs} to $K_d(PAR)$ was calculated according to the references (Brandao et al., 2017; Kirk, 1976; Pierson et al., 2008; Pope & Fry, 1997). The second approach was to establish links between $K_d(PAR)$ and a_{OACs}

in lakes using in situ measured values of all sampling points. Third, regression tree analysis was used to classify the lakes based on $K_d(\text{PAR})$ values, and the relationships between $K_d(\text{PAR})$ and a_{OACs} in different types of lakes were explored using the multivariate regression analysis.

3. Results

3.1 General surface water properties of lakes in different limnetic regions

We analyzed the transparency and trophic status of these sampling lakes, and found that lakes in the YGR had the highest transparency, followed by YGR, MXR, ER, and NER showed the lowest transparency (SDD median/mean \pm standard deviation: 0.40/0.90 \pm 1.03 m) (Fig. 2a). The lakes in NER were highly turbid. NER is in the fluvial plains, the most of lakes in this area are shallow (2.8 \pm 1.8 m) with re-suspension of bottom sediments. The trophic status of lakes across different limnetic regions showed that 24.14% studied lakes in NER had a mesotrophic status, and others were all eutrophic lakes (75.86%). The proportion of eutrophication of NER lakes was the highest in five limnetic regions, followed by ER (65.67%) (Fig. 2b). Agricultural non-point pollution combined with industrial and domestic sewage discharge were the main reasons for these highly eutrophic waters in the NER and ER.

Compared with MXR, lakes in the YGR were more transparent (1.73/2.46 \pm 2.48 m) (Fig. 2a). It is possible that most of the lakes in the YGR are deeper tectonic ones (average: 13.8 m). Lakes in the eastern part of Inner Mongolia were shallow, and strong wind caused re-suspension, resulting in the water turbidity. In these limnetic regions, most of lakes were mesotrophic (>50%), only a few lakes were oligotrophic (<10%) (Fig. 2b). Lakes from the TQR are usually tectonic origins with a larger water depth (21.7 \pm 16.8 m), they are more transparent (3.60/4.69 \pm 3.62 m). Because of less human activities and limited agricultural non-point pollution, the studied lakes in this regions

did not show eutrophication, over half of the sampling waters were oligotrophic (51.72%), and others were all mesotrophic status (48.48%) (Fig. 2b).

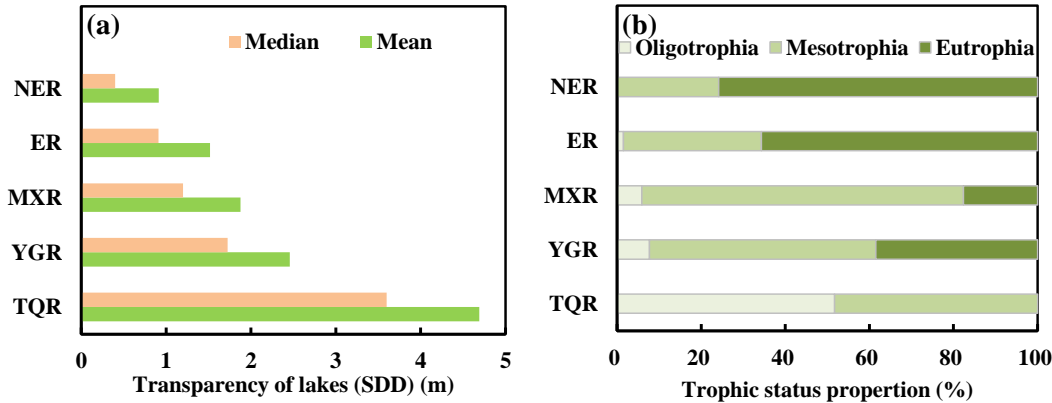


Fig. 2 Analysis of transparency and trophic status of lakes in China's five limnetic regions. (a) the transparency analysis; (b) trophic status analysis.

3.2 Spatial distribution of $K_d(\text{PAR})$

Due to the diverse geographical environments in the area of study, the sampled lakes included the varying $K_d(\text{PAR})$ values (Fig. 1). $K_d(\text{PAR})$ values in different lakes ranged from 0.11-13.93 m^{-1} with the mean of 1.99 m^{-1} . The minimum value occurred in the Pumoyum Co Lake of the southern Tibetan Plateau region. The maximum value occurred in the Qingnian reservoir of Northeastern region. The average $K_d(\text{PAR})$ value for each of the five lake groups was calculated and ranged from 0.60 m^{-1} in TQR to 3.17 m^{-1} in NER (Fig. 3). In NER, the minimum value occurred in the Hengren reservoir of 0.47 m^{-1} . In ER, the minimum value occurred in Haicang Lake of 0.20 m^{-1} . In MXR, the minimum value occurred in Sayram Lake of 0.13 m^{-1} . In YGR, the minimum value occurred in Fuxian Lake of 0.25 m^{-1} . In TQR, the minimum value occurred in Pumoyum Co Lake of 0.11 m^{-1} .

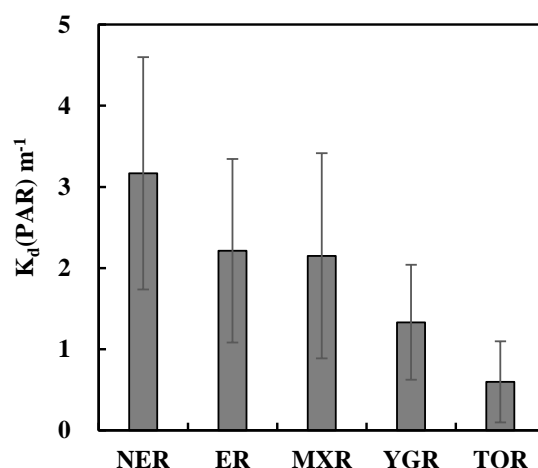
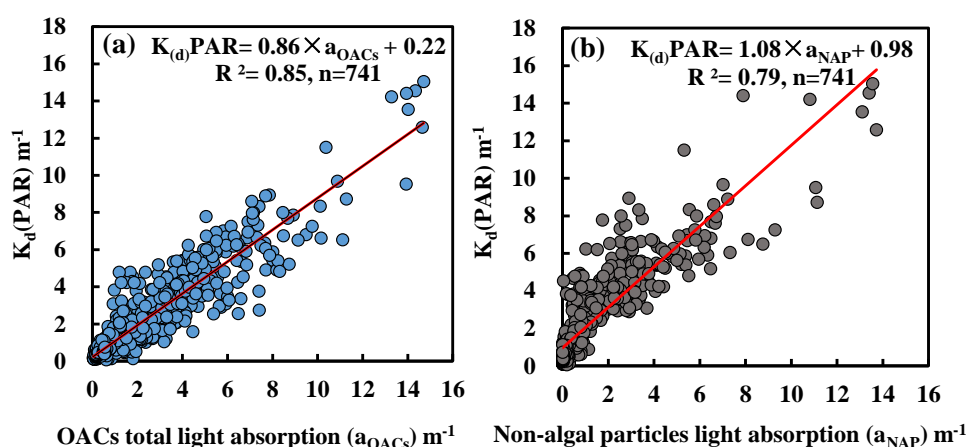


Fig. 3 Compare of mean $K_d(\text{PAR})$ values in five limnetic regions

3.3 Relationship between $K_d(\text{PAR})$ and OACs light absorption

A significant positive correlation was observed between $K_d(\text{PAR})$ and OACs total light absorption in lakes across China at all sampling points, data were evenly distributed on both sides of the regression line (Fig. 4a). The best function to describe the relationship through a linear model: $K_d(\text{PAR}) = 0.86 \times a_{\text{OACs}} + 0.22$ ($R^2 = 0.85$, $n = 741$). The linking between $K_d(\text{PAR})$ and light absorption of each optically active component was also explored. Except a_{NAP} showed a significant positive correlation with $K_d(\text{PAR})$ (Fig. 4b), they all had no significant linear relationship to $K_d(\text{PAR})$ (Fig. 4c-4d).



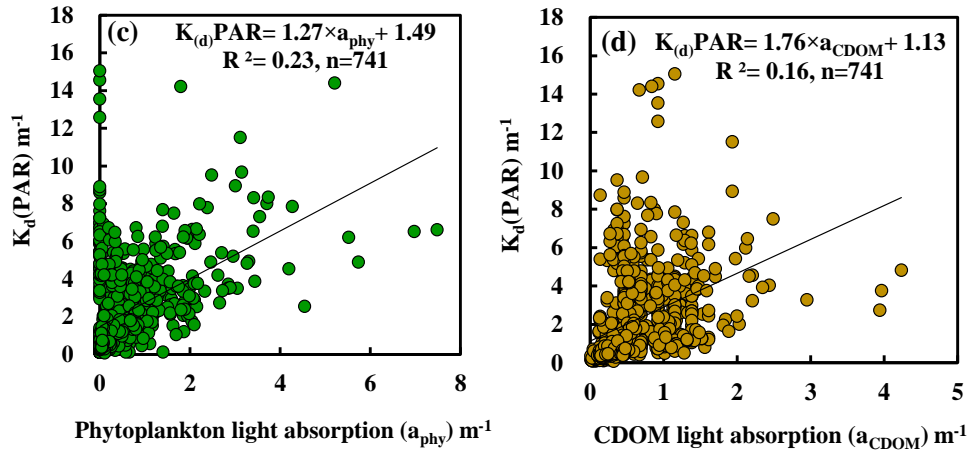


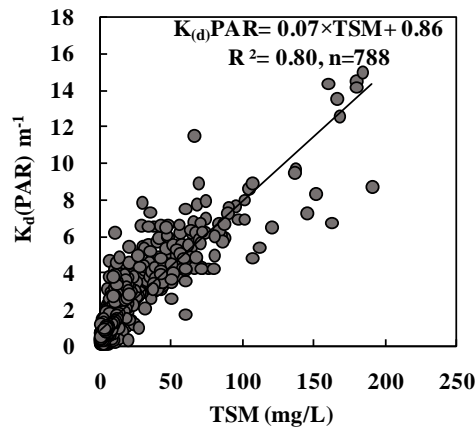
Fig. 4 Scatter plots of diffuse attenuation vs light absorption of optically active components, (a) aOACs, (b) a_{NAP}, (c) a_{phy}, and (d) a_{CDOM}

The result of multiple regression analysis showed that all the optically active components had impact on $K_d(\text{PAR})$, and the relational expression was as follow: $K_d(\text{PAR}) = 0.41 + 0.57 \times a_{\text{CDOM}} + 0.96 \times a_{\text{NAP}} + 0.57 \times a_{\text{phy}}$ ($R^2 = 0.87$, $n = 741$, $p < 0.001$) (Table 1). The standardized coefficient of independent variables indicated that a_{NAP} had the most significant impact on $K_d(\text{PAR})$, followed by a_{phy} . TSM expresses the total concentration of inorganic and pigment particulate matter in water (Budhiman et al., 2012). The relationship between $K_d(\text{PAR})$ and TSM was also explored to support the regression analysis result (Fig. 5).

Table 1 Summary of multiple regression analysis

	R	R Square	Adjusted R Square	Std. Error of the Estimate	Sig.
All lakes	0.931	0.867	0.866	0.833	0.000
TSM <3.8 mg/L	0.863	0.744	0.742	0.220	0.000
TSM >3.8 mg/L (Non-eutrophic lakes)	0.880	0.774	0.770	0.429	0.000
TSM >3.8 mg/L (Eutrophic lakes)	0.874	0.764	0.762	1.106	0.000

264 Dependent Variable: $K_d(\text{PAR})$; Predictors: constant, a_{phy} , a_{NAP} , a_{CDOM}



266 Fig. 5 Relationship between $K_d(\text{PAR})$ and total suspended matter concentration (TSM)

267 In five limnetic regions, the significant positive correlation was also observed
 268 between $K_d(\text{PAR})$ and total light absorption of OACs (Fig. 6). The relationship
 269 coefficient and fitting degree (R^2) all changed for lakes in different limnetic regions.
 270 The regression model in TQR had the best fitting degree ($R^2 = 0.85$) and the greatest
 271 relationship coefficient (slope=0.95) than in other limnetic regions. In MXR, the
 272 regression model was $K_d(\text{PAR}) = 0.79 \times a_{\text{OACs}} + 0.08$ ($R^2 = 0.81$, $n = 156$) with the smallest
 273 relationship coefficient. In YGR, the regression model was $K_d(\text{PAR}) = 0.82 \times a_{\text{OACs}} + 0.33$
 274 ($R^2 = 0.80$, $n = 156$) with the lowest fitting degree.

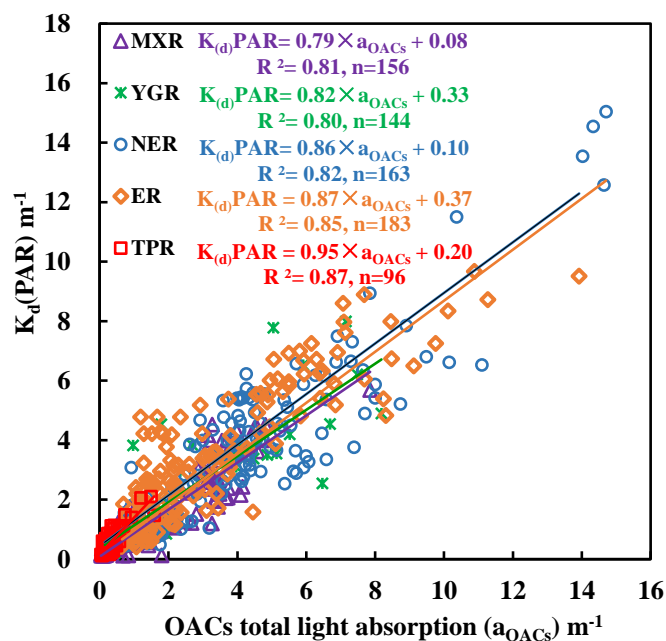


Fig. 6 Relationships between $K_d(\text{PAR})$ and a_{OACs} in five limnetic regions

In all limnetic regions in this study, $K_d(\text{PAR})$ was dominated by inorganic particulate matter absorption/scattering, followed by pigment particulate matters in all limnetic regions with mean relative contributions of 57.95% and 28.20%, respectively. The highest mean relative contribution of inorganic particulate matter to $K_d(\text{PAR})$ (71.55 %) was in highest YGR, followed by NER (64.17 %), TQR (59.35 %), MXR (48.26 %), and ER (46.45 %) (Fig. 7). There is a little part of the $K_d(\text{PAR})$ variation could be explained by CDOM with the contributions in YGR of 6.78%, in NER of 9.99%, in TQR of 10.38%, in MXR of 11.75%, and in ER of 8.71% (Fig. 7).

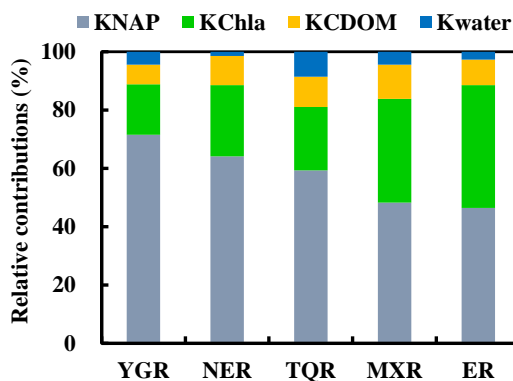


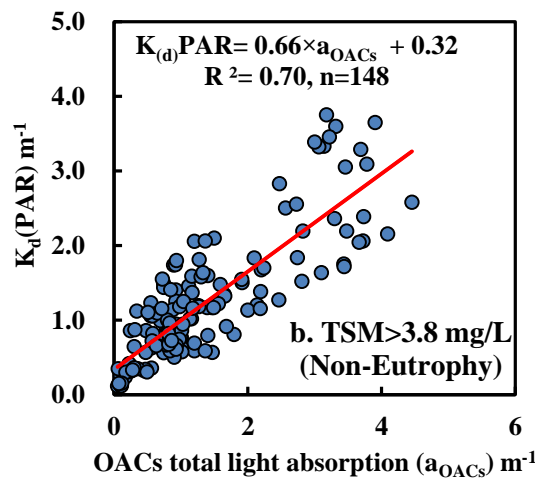
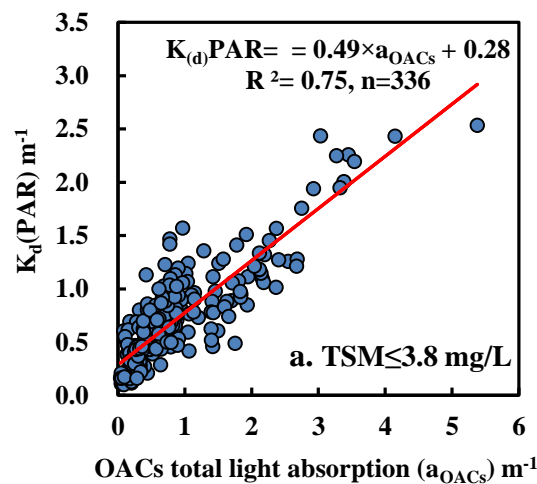
Fig. 7 Relative contributions of OACs to $K_d(\text{PAR})$. K_{water} is the partial attenuation coefficient by pure water, K_{CDOM} by CDOM, K_{NAP} by inorganic suspended particles, and K_{Chla} by pigment particles

3.4 Relationship between $K_d(\text{PAR})$ and a_{OACs} in different lakes

Regression tree analysis showed this pattern of $K_d(\text{PAR})$ was mainly affected by TSM concentration in these inland lakes. The $K_d(\text{PAR})$ values in these lakes could be divided into two branches having a TSM threshold of 3.8 mg/L. When the TSM concentration of water was lower than 3.8 mg/L, the TSM concentration was the only predictive factor for $K_d(\text{PAR})$ values. However, the $K_d(\text{PAR})$ value in lakes with the TSM concentration higher than 3.8 mg/L, was also affected by trophic status. $K_d(\text{PAR})$ value in oligo- and Meso- trophic waters (mean \pm SD: $1.26 \pm 0.89 \text{ m}^{-1}$) was lower than in eutrophic waters

(mean \pm SD: 4.59 \pm 2.18 m⁻¹). From this point forward, the lakes are divided into two types used 3.8 mg/L TSM concentration as a threshold: low TSM lakes and high TSM lakes.

In order to specify the model applicability, the relationship between $K_d(\text{PAR})$ and a_{OACs} was also analyzed established for the lakes with different TSM concentration and trophic status. The regression model for lakes with low TSM had a lower slope (slope =0.49) than lakes with high TSM (slope =0.66, slope =0.73) with a good fitting degree (R^2) (Fig. 8). However, the relationship coefficient and R^2 all changed for lakes with different trophic status. In the oligo- and Meso- trophic waters (non-eutrophy), the R^2 attained 0.70 with the relationship coefficient 0.66 (Fig. 8). In the eutrophic waters, the regression model was $K_d(\text{PAR})=0.73 \times a_{\text{OACs}}+1.04$ with the R^2 of 0.72 (Fig. 8).



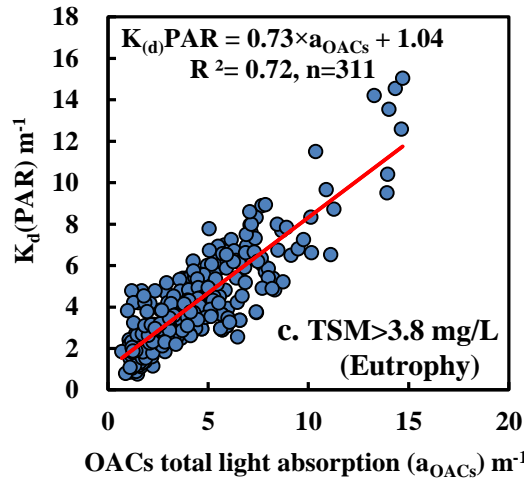


Fig. 8 Relationships between $K_d(\text{PAR})$ and a_{OACs} in different lakes

In the waters with low TSM, the result of multiple regression analysis showed a_{CDOM} had the most significant impact on $K_d(\text{PAR})$, followed by a_{NAP} , the relational expression was $K_d(\text{PAR}) = 0.30 + 0.48 \times a_{\text{CDOM}} + 0.72 \times a_{\text{NAP}} + 0.20 \times a_{\text{phy}}$ ($R^2 = 0.74$, $p < 0.001$) (Table 1). In the waters with high TSM, the multiple regression analysis indicated that not all the OACs had impact on $K_d(\text{PAR})$ in oligo- and Meso- trophic waters. a_{phy} was excluded during the building of regression model. The relational expression was as follow: $K_d(\text{PAR}) = 0.56 + 0.51 \times a_{\text{CDOM}} + 0.52 \times a_{\text{NAP}}$ ($R^2 = 0.77$, $p < 0.001$) (Table 1). The standardized coefficient of independent variables indicated that a_{CDOM} had more impact on $K_d(\text{PAR})$ than a_{NAP} in these non-eutrophic waters. In eutrophic waters with high TSM, the regression model was $K_d(\text{PAR}) = 1.47 + 0.35 \times a_{\text{CDOM}} + 0.82 \times a_{\text{NAP}} + 0.41 \times a_{\text{phy}}$ ($R^2 = 0.76$, $p < 0.001$) (Table 1). a_{NAP} had the most significant impact on $K_d(\text{PAR})$, followed by a_{phy} .

4. Discussion

4.1 $K_d(\text{PAR})$ in different limnetic regions of China

In the present study, 47.37% of the in situ $K_d(\text{PAR})$ values ranged from 0.11 m^{-1} to 1.00 m^{-1} , and 43.61% of $K_d(\text{PAR})$ ranged from 1.00 m^{-1} to 5.00 m^{-1} , reflecting that approximately half of these lakes are the turbid water body. The comparison of the

average $K_d(\text{PAR})$ value in the five limnetic regions indicated that the lakes in TQR were the most clear water, and the lakes in NER were the most turbid water (Fig. 3a). The lake area in TQR accounts for 51.4% of total China lake area, and the majority of TQR lakes are closed lakes with high salinity and low temperature (Ma et al., 2011; Song et al., 2018). The lacustrine environment in TQR is suffered less interference from anthropogenic activity with little allochthonous nutrient. The algae growth is few due to the high salinity, low temperature, and low nutrient input, accompanying with low Chla concentration. Moreover, the strong ultraviolet radiation in TQR could cause CDOM photolysis and photobleaching in waters, resulting in low CDOM absorption (Shang et al., 2018). Many large and medium-sized lakes in TQR, developed in intermontane basin or longitudinal valley, are the tectonic lake with deep water and steep shore. The TSM concentration in these deep lakes may be not significantly influenced by surface runoff and wind disturbance. According to the above reasons, the lakes in TQR may have a high water transparency, and the attenuation of light may be relatively few than other limnetic regions. Previous study has pointed out that most of lakes in NER were shallow lakes (Song et al., 2013), and in shallow lakes, TSM usually plays a noticeable impact on the attenuation of light and water transparency (Pierson et al., 2003; Shi et al., 2014; Van Duin et al., 2001). TSM concentration is always higher in the shallow lakes due to the sediment re-suspension driven by wave disturbance (Shi et al., 2014). A lake's susceptibility to sediment re-suspension induced by wind-driven waves can be estimated by a dynamic ratio index of 0.8 km/m (the square root of the surface area divided by the average depth) (Bachmann et al., 2000). We calculated the dynamic ratios for the lakes in NER, results showed that the values ranged from 0.82 to 10.16 km/m . All lakes in NER in this study exceeded the critical value, which supported that the resuspension driven by winds happened in these NER lakes. The

higher TSM concentration led to the water turbidity and high $K_d(\text{PAR})$ value. These results were similar to those for other shallow, turbid, inland waters (Shi et al., 2014; Song et al., 2017; Zheng et al., 2016).

The $K_d(\text{PAR})$ in the water is determined by pure water and OACs, but the main deciding factor may be different in different environments and lakes. The relative contributions of OACs showed $K_d(\text{PAR})$ was dominated by inorganic particulate matter absorption/scattering in all limnetic regions in this study (Fig. 7), the findings are similar to previous findings on inland water bodies (Devlin et al., 2009; Ma et al., 2016; Shi et al., 2014; Zhang et al., 2007a). However, there were marked regional differences in the relative roles of inorganic particulate matter, Chl-*a* and CDOM to $K_d(\text{PAR})$ (Fig. 7). The highest relative contribution of inorganic particulate matter was presented in YGR (Fig. 7). In this study, most of the studied lakes in the YGR are tectonic ones with the mean deep more 10 m. The seasonal water layering is a universal phenomenon in deep lakes (Ndebele-Murisa et al., 2014; Wetzel, 2001). Previous studies have been demonstrated that mixing of the water column caused resuspension of particulate matter increasing inorganic particulate matter concentrations (!!! INVALID CITATION !!!), which may explain the highest average contribution of inorganic particulate matter to $K_d(\text{PAR})$ (71.55%) in the YGR lakes. Most of the studied lakes in YGR, over 60%, was mesotrophic with the lower Chl*a* concentration, except a few highly eutrophic lakes, such as Dianchi Lake and Xingyun Lake. The algae and phytoplankton existed with an appropriate biomass, and pigment particulate matter only had a weak contribution to $K_d(\text{PAR})$. The strong photobleaching and photodegradation by intensive ultraviolet radiation in YGR have destroyed CDOM structure and weakened CDOM light absorption, resulting in the minimum contribution to $K_d(\text{PAR})$. The same phenomenon occurred in TQR (Fig. 7). However, in ER, the relative contributions of Chl*a* to $K_d(\text{PAR})$

is nearly equal to the inorganic particulate matter. ER situated in the fluvial plains, and most lakes were shallow (2.8 ± 1.8 m), the waters always have high concentrations of suspended particulate matter due to the re-suspension of bottom sediments and inflow of surface runoff (Bachmann et al., 2000; Zhang et al., 2007b). Waters in the ER are highly turbid with a very low transparency (0.4 ± 0.3 m). Meanwhile, the relatively high concentrations of nutrients (TN: 0.94 ± 1.31 mg/L, and TP: 0.32 ± 1.02 mg/L) in lakes resulted in phytoplankton overgrowth, even bloom. 85% of the studied lakes in the ELR was eutrophic or hyper-eutrophic according to Carlson's trophic index (Carlson, 1977), the pigment particulate matter during the algae decomposes and metabolism was released to water. Many studies have proven that the controlling factor of $K_d(\text{PAR})$ was different with variation of the region (Zheng et al., 2016). Despite Chla and CDOM contributed to $K_d(\text{PAR})$ in ER and MXR lakes, inorganic particulate matter was largely responsible for the attenuation. The relationships coefficient and fitting degrees (R^2) between $K_d(\text{PAR})$ and a_{OACs} all changed in different limnetic regions, which further veriflicated indicate that the deciding factor of $K_d(\text{PAR})$ was different. This study have indicated that althouth it sometimes had the same decisiving factor of $K_d(\text{PAR})$ in different regions, the relative contributions of OACs to $K_d(\text{PAR})$ still had a huge difference.

4.2 Influence of OACs absorption on $K_d(\text{PAR})$ in lakes

OACs have the deciding effect on $K_d(\text{PAR})$ value (Shi et al., 2014). In this study, either in five limnetic regions or different trophic lakes, the OACs absorption and $K_d(\text{PAR})$ had a significantly positive correlation, a_{OACs} could explain 70%-87% of $K_d(\text{PAR})$ variations (Fig 5, Fig. 8). In the whole sduty area, a_{NAP} was the most significantly regulating factor on $K_d(\text{PAR})$. The determination coefficient between $K_d(\text{PAR})$ and a_{NAP} ($R^2 = 0.79$) was significantly higher than that between $K_d(\text{PAR})$ and a_{phy} , and between

$K_d(\text{PAR})$ and a_{CDOM} ($R^2=0.23$, $R^2=0.16$) (Fig. 4b-d). However, there are marked differences in the relative contributions of a_{OACs} to light attenuation in different waters (Belzile et al., 2002; Brandao et al., 2017; Philips et al., 1995a; V-Balogh et al., 2009).

When the lakes were divided into different groups by TSM concentration in this study, the determining factor of $K_d(\text{PAR})$ changed with the lake type. In the lakes with low TSM concentration and non-eutrophic lakes with high TSM, a_{CDOM} was the most powerful factor on $K_d(\text{PAR})$, followed by a_{NAP} . The relative contribution analysis of CDOM, Chla, and inorganic particulate matters to the total non-water light absorption was conducted in these waters, and the results indicated that at most of these sampling waters, CDOM absorption played a major role on total non-water light absorption, and Chla played a minor role. These waters can be classified as “CDOM-type” water according to the optical classification of surface waters (Prieur & Sathyendranath, 1981). Studies have indicated that in most of the highly colored inland waters, CDOM had a dominating influence on light attenuation, reducing the amount of PAR many-fold (Kirk, 1976; V-Balogh et al., 2009). Besides, the strong correlations between $K_d(\text{PAR})$ and TSM also implied that light attenuation in the lakes with high TSM concentration, the particulate absorption, including a_{NAP} and a_{phy} , had an indispensable influence on $K_d(\text{PAR})$ (Fig. 5). But within the PAR waveband, CDOM absorbs maximally in the blue region of the spectrum in many natural waters (Frankovich et al., 2017; Markager & Vincent, 2000; Morris et al., 1995). CDOM absorption overlaps the blue absorption maximum for Chla, which affected the light availability of phytoplankton, resulting in the low Chla concentration and the low contribution of a_{phy} to $K_d(\text{PAR})$ (Markager & Vincent, 2000).

In eutrophic lakes with high TSM, a_{NAP} had the most significant impact on $K_d(\text{PAR})$, followed by a_{phy} . In fact, the low contribution of a_{CDOM} to $K_d(\text{PAR})$ has been

predicted since the a_{CDOM} occupied a low proportion in a_{OAC} (Mean \pm SD: $24.30 \pm 14.97\%$) in this type of lakes. These waters can be classified as “NAP-type” water with high TSM contrations (Mean \pm SD: 40.94 ± 35.50 mg/L) and high proportion of a_{NAP} to a_{OAC} (Mean \pm SD: $51.19 \pm 22.87\%$) (Prieur & Sathyendranath, 1981). The concentration of calcite particles was the most important factor regulating summer light attenuation within Otisco Lake, New York (Weidemann et al., 1985). In Japan Lake Biwa with bloom-forming cyanobacteria, researchers also found that particulate absorption played significant roles to $K_d(PAR)$ than a_{CDOM} (Belzile et al., 2002). The re-suspension of bottom sediments caused by strong winds in autumn correlated with high $K_d(PAR)$ values, which was because of the high inorganic particles matters concentration (Ma et al., 2016; Song et al., 2017). However, in these turbid waters, the trophic status or Chla concentration also had important influence on light attenuation (Effler et al., 1985). Studies have pointed out that the effect of sediments re-suspension caused by strong wind on $K_d(PAR)$ could be disturbed by the high phytoplankton concentration in spring and summer, the algal bloom in lakes increased the contribution of Chla to $K_d(PAR)$ (Song et al., 2017). The research on hypertrophic waters in Hungary indicated that a_{phy} played an important role in the PAR attenuation (V-Balogh et al., 2009). Results of this study are suggesting that new studies on the variability of $K_d(PAR)$ in inland waters must consider the hydrodynamic conditions, trophic status and the distribution of OACs within the waters (Brandao et al., 2017).

The $K_d(PAR)$ in the water is governed by absorption and scattering of water, CDOM, and particulate matter (Ma et al., 2016; Song et al., 2017; Zheng et al., 2016), the pure water effects are always regarded as the background value of $K_d(PAR)$, so the absorption and scattering of OACs have the deciding effect on $K_d(PAR)$ value (Shi et al., 2014). In this study, only the contribution of OACs absorption on $K_d(PAR)$ was

analyzed and discussed. The absorption of OACs directly attenuated the photo energy without change of light transmission direction, but the scattering of particles matters changed light transmission direction, which resulted in the change of light absorption along the initial transmission direction (Budhiman et al., 2012; Kirk, 1976; Zheng et al., 2016). In fact, a_{OACs} could explain most of $K_d(PAR)$ variations (Fig 5, Fig. 8), the scattering contribution of particles matters to $K_d(PAR)$ variations in natural waters was relatively small (Belzile et al., 2002; Lund-Hansen, 2004). The previous studies have found that scattering of particles matters decreased approximately linearly with increasing wavelength in particle dominated natural waters (Haltrin, 1999; Morel & Loisel, 1998; Pegau et al., 1999). Most of the lakes in this study had the high suspended particles concentration, so the effect of scattering on $K_d(PAR)$ variations may be very weak. Due to the limitation of the our experimental conditions, the scattering of particles matters did not measured in this study, a detailed in situ profiles of spectral absorption and attenuation measured using the AC-9 may help us to understand the results of the research.

5. Conclusions

The spatial distribution of average $K_d(PAR)$ in five limnetic regions China showed that the minimum value in TQR (0.60 ± 0.99 and the maximum in NER ($3.17 \pm 2.86 \text{ m}^{-1}$). The inorganic particulate matters had the highest average relative contribution to $K_d(PAR)$ (57.95%).

The a_{OACs} could explain 70%-87% of $K_d(PAR)$ variations with the following relationship: $K_d(PAR) = 0.41 + 0.57 \times a_{CDOM} + 0.96 \times a_{NAP} + 0.57 \times a_{phy}$ ($R^2 = 0.87$, $n = 741$, $p < 0.001$). However, the influence of different components of a_{OACs} on $K_d(PAR)$ changed with the lake type. In the lakes with low TSM concnetration and non-eutrophic lakes with high TSM, a_{CDOM} was the most powerful factor on $K_d(PAR)$. In eutrophic

lakes with high TSM, a_{NAP} had the most significant impact on $K_d(PAR)$, followed by a_{phy} . A precise understanding the effect of OACs absorption on $K_d(PAR)$ is essential to remote sensing of water color and evaluate the underwater light climate.

Acknowledgments

This study was jointly supported by the National Natural Science Foundation of China (No. 41730104, No. 41701423), the “One Hundred Talents Program” of the Chinese Academy of Sciences granted to Kaishan Song, 13th Five-Year Plan of Technical and Social Research Project for Jilin Colleges (JJKH20170257KJ), and Jilin Scientific & Technological Development Program (No. 20160520075JH).

References

- Aizaki, M., Otsuki, A., Fukushima, T., Kawai, T., Hosomi, M., Muraoka, K. Application of modified Carlson's trophic state index to Japanese lakes and its relationship to other parameters related to trophic state. Research report of National Institute of environmental study. 1981.
- APHA, AWWA, WEF. 1998. Standard methods for the examination of water and wastewater, American Public Health Association. Washington, DC.
- Bachmann, R. W., Hoyer, M. V., Canfield, D. E.: The Potential For Wave Disturbance in Shallow Florida Lakes, *Lake Reserv. Manage.*, 16(4), 281-291, 2000.
- Belzile, C., Vincent, W. F., Kumagai, M.: Contribution of absorption and scattering to the attenuation of UV and photosynthetically available radiation in Lake Biwa, *Limnol. Oceanogr.*, 47(1), 95-107, 2002.
- Brandao, L. P. M., Brighenti, L. S., Staehr, P. A., Barbosa, F. A. R., Bezerra-Neto, J. F.: Partitioning of the diffuse attenuation coefficient for photosynthetically available irradiance in a deep dendritic tropical lake, *Anais Da Academia Brasileira De Ciencias*, 89(1), 469-489, 2017.
- Breiman, L., Friedman, J., Olshen, R.: Classification and Regression Trees. Wadsworth International Group, Belmont. 1984.
- Bricaud, A., Morel, A., Prieur, L.: Absorption by dissolved organic matter of the sea (Yekkow substance) in the UV and visible domains, *Limnol. Oceanogr.*, 26(1), 43-53, 1981.
- Bricaud, A., Stramski, D.: Spectral absorption coefficients of living phytoplankton and nonalgal biogenous matter: A comparison between the Peru upwelling area and the Sargasso Sea, *Limnol. Oceanogr.*, 35(3), 562-582, 1990.
- Budhiman, S., Suhyb Salama, M., Vekerdy, Z., Verhoef, W.: Deriving optical properties of Mahakam Delta coastal waters, Indonesia using in situ measurements and ocean color model inversion, *ISPRS J. Photogramm. Remote Sens.*, 68, 157-169, 2012.
- Carlson, R. E.: A trophic state index for lakes, *Limnol. Oceanogr.*, 22(2), 361-369, 1977.

513 Chen, J., Zhu, Y., Wu, Y., Cui, T., Ishizaka, J., Ju, Y.: A Neural Network Model for K(λ) Retrieval
514 and Application to Global K-par Monitoring, PLoS One 10(6), 2015.

515 Cleveland, J. S., Weidemann, A. D.: Quantifying absorption by aquatic particles: A multiple scattering
516 correction for glass-fiber filters, Limnol. Oceanogr., 38(6), 1321-1327, 1993.

517 Cunningham, A., Ramage, L., McKee, D.: Relationships between inherent optical properties and the
518 depth of penetration of solar radiation in optically complex coastal waters, Journal of
519 Geophysical Research-Oceans, 118(5), 2310-2317, 2013.

520 Devlin, M. J., Barry, J., Mills, D. K., Gowen, R. J., Foden, J., Sivyver, D., Greenwood, N., Pearce, D.,
521 Tett, P.: Estimating the diffuse attenuation coefficient from optically active constituents in UK
522 marine waters, Estuar. Coast. Shelf Sci., 82(1), 73-83, 2009.

523 Devlin, M. J., Barry, J., Mills, D. K., Gowen, R. J., Foden, J., Sivyver, D., Tett, P.: Relationships between
524 suspended particulate material, light attenuation and Secchi depth in UK marine waters, Estuar.
525 Coast. Shelf Sci., 79(3), 429-439, 2008.

526 Effler, S. W., Schafran, G. C., Driscoll, C. T.: Partitioning Light Attenuation in an Acidic Lake, Can. J.
527 Fish. Aquat. Sci., 42(11), 1707-1711, 1985.

528 Frankovich, T. A., Rudnick, D. T., Fourqurean, J. W.: Light attenuation in estuarine mangrove lakes,
529 Estuarine Coastal and Shelf Science, 184, 191-201, 2017.

530 Haltrin, V. I.: Chlorophyll-based model of seawater optical properties, Appl. Opt., 38(33), 6826-6832,
531 1999.

532 Hampton, S. E., Galloway, A. W. E., Powers, S. M., et al. Ecology under lake ice. Ecol. Lett., 20: 98-111,
533 2017.

534 Jeffrey, S. W., Humphrey, G. F.: New spectrophotometric equations for determining chlorophylls a, b, c1
535 and c2 in higher plants, algae and natural phytoplankton, Biochemie und Physiologie der
536 Pflanzen, 167(2), 191-194, 1975.

537 Jin, X. C., Xu, Q. J., Huang, C. Z.: Current status and future tendency of lake eutrophication in China,
538 Science in China Series C-Life Sciences, 48, 948-954, 2005.

539 Kirk, J. T. O. 1994. *Light and Photosynthesis in Aquatic Ecosystems*. Cambridge University Press, UK.

540 Kirk, J. T. O.: Yellow substance (gelbstoff) and its contribution to the attenuation of photosynthetically
541 active radiation in some inland and coastal south-eastern Australian waters, Australian Journal
542 of Marine and Freshwater Research, 27(1), 61-71, 1976.

543 Laurion, I., Ventura, M., Catalan, J., Psenner, R., Sommaruga, R.: Attenuation of ultraviolet radiation in
544 mountain lakes: Factors controlling the among- and within-lake variability, Limnol. Oceanogr.,
545 45(6), 1274-1288, 2000.

546 Lund-Hansen, L. C.: Diffuse attenuation coefficients K-d(PAR) at the estuarine North Sea-Baltic Sea
547 transition: time-series, partitioning, absorption, and scattering, Estuarine Coastal and Shelf
548 Science, 61(2), 251-259, 2004.

549 Ma, J., Song, K., Wen, Z., Zhao, Y., Shang, Y., Fang, C., Du, J.: Spatial Distribution of Diffuse
550 Attenuation of Photosynthetic Active Radiation and Its Main Regulating Factors in Inland
551 Waters of Northeast China, Remote Sensing, 8(11), 2016.

552 Ma, R., Yang, G., Duan, H., Jiang, J., Wang, S., Feng, X., Li, A., Kong, F., Xue, B., Wu, J., Li, S.: China's
553 lakes at present: Number, area and spatial distribution, Science China Earth Science, 41(3), 394-
554 401, 2011.

555 Markager, S., Vincent, W. F.: Spectral light attenuation and the absorption of UV and blue light in natural
556 waters, Limnol. Oceanogr., 45(3), 642-650, 2000.

557 Matsushita, B., Yang, W., Yu, G., Oyama, Y., Yoshimura, K., Fukushima, T.: A hybrid algorithm for
558 estimating the chlorophyll-a concentration across different trophic states in Asian inland waters,
559 ISPRS J. Photogramm. Remote Sens. , 102, 28-37, 2015.

560 Morel, A., Loisel, H.: Apparent optical properties of oceanic water: dependence on the molecular
561 scattering contribution, Appl. Opt., 37(21), 4765-4776, 1998.

562 Morris, D. P., Zagarese, H., Williamson, C. E., Balseiro, E. G., Hargreaves, B. R., Modenutti, B., Moeller,
563 R., Queimalinos, C.: The attenuation of solar UV radiation in lakes and the role of dissolved
564 organic carbon, Limnol. Oceanogr., 40(8), 1381-1391, 1995.

565 Ndebele-Murisa, M. R., Musil, C. F., Magadza, C. H. D., Raitt, L.: A decline in the depth of the mixed
566 layer and changes in other physical properties of Lake Kariba's water over the past two decades,
567 Hydrobiologia, 721(1), 185-195, 2014.

568 Oliver, S. K., Collins, S. M., Soranno, P. A., Wagner, T., Stanley, E. H., Jones, J. R., Stow, C. A., Lottig,
569 N. R.: Unexpected stasis in a changing world: Lake nutrient and chlorophyll trends since 1990,
570 Global Change Biol., 23(12), 5455-5467, 2017.

571 Pegau, W. S., Zaneveld, J. R. V., Barnard, A. H., Maske, H., Alvarez-Borrego, S., Lara-Lara, R.,
572 Cervantes-Duarte, R.: Inherent optical properties in the Gulf of California, Cienc. Mar., 25(4),
573 469-485, 1999.

574 Philips, E. J., Aldridge, F. J., Schelske, C. L., Crisman, T. L.: RELATIONSHIPS BETWEEN LIGHT
575 AVAILABILITY, CHLOROPHYLL-A, AND TRIPTON IN A LARGE, SHALLOW
576 SUBTROPICAL LAKE, Limnol. Oceanogr., 40(2), 416-421, 1995a.

577 Philips, E. J., Lynch, T. C., Badylak, S.: Chl-a, tripton, color, and light availability in a shallow tropical
578 inner-shelf lagoon, Mar. Ecol. Prog. Ser., 127(1-3), 223-234, 1995b.

579 Pierson, D. C., Kratzer, S., Strombeck, N., Hakansson, B.: Relationship between the attenuation of
580 downwelling irradiance at 490 nm with the attenuation of PAR (400 nm-700 nm) in the Baltic
581 Sea, Remote Sens. Environ., 112(3), 668-680, 2008.

582 Pierson, D. C., Markensten, H., Strömbeck, N. 2003. Long and short term variations in suspended
583 particulate material: the influence on light available to the phytoplankton community. *The*
584 *Interactions between Sediments and Water*, 2003//, Dordrecht. Springer Netherlands. pp. 299-
585 304.

586 Pope, R. M., Fry, E. S.: Absorption spectrum (380-700 nm) of pure water .2. Integrating cavity
587 measurements, Appl. Opt., 36(33), 8710-8723, 1997.

588 Prieur, L., Sathyendranath, S.: An optical classification of coastal and oceanic waters based on the
589 specific spectral absorption curves of phytoplankton pigments, dissolved organic matter, and
590 other particulate materials, Limnol. Oceanogr., 26(4), 671-689, 1981.

591 Raymond, P. A., Hartmann, J., Lauerwald, R., Sobek, S., McDonald, C., Hoover, M., Butman, D., Striegl,
592 R., Mayorga, E., Humborg, C., Kortelainen, P., Duerr, H., Meybeck, M., Ciais, P., Guth, P.:
593 Global carbon dioxide emissions from inland waters, Nature, 503(7476), 355-359, 2013.

594 Shang, Y., Song, K., Wen, Z., Lyu, L., Zhao, Y., Fang, C., Zhang, B.: Characterization of CDOM
595 absorption of reservoirs with its linkage of regions and ages across China, Environ. Sci. Pollut.
596 Res., 2018.

597 Shi, K., Zhang, Y., Liu, X., Wang, M., Qin, B.: Remote sensing of diffuse attenuation coefficient of
598 photosynthetically active radiation in Lake Taihu using MERIS data, Remote Sens. Environ.,
599 140, 365-377, 2014.

600 Song, K., Ma, J., Wen, Z., Fang, C., Shang, Y., Zhao, Y., Wang, M., Du, J.: Remote estimation of K-d

(PAR) using MODIS and Landsat imagery for turbid inland waters in Northeast China, ISPRS J. Photogramm. Remote Sens. , 123, 159-172, 2017.

Song, K., Wen, Z., Shang, Y., Yang, H., Lyu, L., Liu, G., Fang, C., Du, J., Zhao, Y.: Quantification of dissolved organic carbon (DOC) storage in lakes and reservoirs of mainland China, J. Environ. Manage., 217, 391-402, 2018.

Song, K. S., Zang, S. Y., Zhao, Y., Li, L., Du, J., Zhang, N. N., Wang, X. D., Shao, T. T., Guan, Y., Liu, L.: Spatiotemporal characterization of dissolved carbon for inland waters in semi-humid/semi-arid region, China, Hydrol. Earth Syst. Sci. , 17(10), 4269-4281, 2013.

Stambler, N.: Bio-optical properties of the northern Red Sea and the Gulf of Eilat (Aqaba) during winter 1999, J. Sea Res., 54(3), 186-203, 2005.

V-Balogh, K., Nemeth, B., Voros, L.: Specific attenuation coefficients of optically active substances and their contribution to the underwater ultraviolet and visible light climate in shallow lakes and ponds, Hydrobiologia, 632(1), 91-105, 2009.

Van Duin, E. H. S., Blom, G., Los, F. J., Maffione, R., Zimmerman, R., Cerco, C. F., Dortch, M., Best, E. P. H.: Modeling underwater light climate in relation to sedimentation, resuspension, water quality and autotrophic growth, Hydrobiologia, 444(1), 25-42, 2001.

Weidemann, A. D., Bannister, T. T., Effler, S. W., Johnson, D. L.: Particulate and optical properties during CaCO_3 precipitation in Otisco Lake, Limnol. Oceanogr., 30(5), 1078-1083, 1985.

Wen, Z., Song, K., Shang, Y., Fang, C., Li, L., Lv, L., Lv, X., Chen, L.: Carbon dioxide emissions from lakes and reservoirs of China: A regional estimate based on the calculated pCO_2 , Atmos. Environ., 170(Supplement C), 71-81, 2017.

Wen, Z. D., Song, K. S., Zhao, Y., Du, J., Ma, J. H.: Influence of environmental factors on spectral characteristics of chromophoric dissolved organic matter (CDOM) in Inner Mongolia Plateau, China, Hydrol. Earth Syst. Sci. , 20(2), 787-801, 2016.

Wetzel, R. G. 2001. *Limnology: Lake and River Ecosystems. Third Edition ed.* Academic Press, California, USA.

Yamaguchi, H., Katahira, R., Ichimi, K., Tada, K.: Optically active components and light attenuation in an offshore station of Harima Sound, eastern Seto Inland Sea, Japan, Hydrobiologia, 714(1), 49-59, 2013.

Yang, H., Xie, P., Xing, Y. P., Ni, L. Y., Guo, H. T.: Attenuation of photosynthetically available radiation by chlorophyll, chromophoric dissolved organic matter, and tripton in lake Donghu, China, J. Freshwat. Ecol., 20(3), 575-581, 2005.

Zhang, Y., Zhang, B., Ma, R., Feng, S., Le, C.: Optically active substances and their contributions to the underwater light climate in Lake Taihu, a large shallow lake in China, Fundamental and Applied Limnology, 170(1), 11-19, 2007a.

Zhang, Y., Zhou, Y., Shi, K., Qin, B., Yao, X., Zhang, Y.: Optical properties and composition changes in chromophoric dissolved organic matter along trophic gradients: Implications for monitoring and assessing lake eutrophication, Water Res., 131, 255-263, 2018.

Zhang, Y. L., Zhang, B., Ma, R. H., Feng, S., Le, C. F.: Optically active substances and their contributions to the underwater light climate in Lake Taihu, a large shallow lake in China, Fundamental and Applied Limnology, 170(1), 11-19, 2007b.

Zhao, Y., Song, K., Wen, Z., Li, L., Zang, S., Shao, T., Li, S., Du, J.: Seasonal characterization of CDOM for lakes in semiarid regions of Northeast China using excitation–emission matrix fluorescence and parallel factor analysis (EEM–PARAFAC), Biogeosciences, 13(5), 1635-1645, 2016.

645 Zheng, Z., Ren, J., Li, Y., Huang, C., Liu, G., Du, C., Lyu, H.: Remote sensing of diffuse attenuation
646 coefficient patterns from Landsat 8 OLI imagery of turbid inland waters: A case study of
647 Dongting Lake, Sci. Total Environ., 573, 39-54, 2016.
648